Journal of
Marine Science and Engineering

MDPI

Article

Methodological Solutions for Predicting Energy Efficiency of Organic Rankine Cycle Waste Heat Recovery Systems Considering Technological Constraints

Sergejus Lebedevas and Tomas Čepaitis *

Faculty of Marine Technology and Natural Sciences, Marine Engineering Department, Klaipeda University, 91225 Klaipeda, Lithuania; sergejus.lebedevas@ku.lt
* Correspondence: tomas.cepaitis@wsy.lt

Abstract: Solving strategic IMO tasks for the decarbonization of maritime transport and the dynamics of its controlling indicators (EEDI, EEXI, CII) involves the comprehensive use of renewable and low-carbon fuels (LNG, biodiesel, methanol in the mid-term perspective of 2030, ammonia, and hydrogen to achieve zero emissions by 2050) and energy-saving technologies. The technology of regenerating secondary heat sources of the ship's power plant WHR in the form of an Organic Rankine Cycle (ORC) is considered one of the most promising solutions. The attractiveness of the ORC is justified by the share of the energy potential of WHR at 45–50%, almost half of which are low-temperature WHR (80–90 °C and below). However, according to DNV GL, the widespread adoption of WHR-ORC technologies, especially on operating ships, is hindered by the statistical lack of system prototypes combined with the high cost of implementation. Developing methodological tools for justifying the energy efficiency indicators of WHR–ORC cycle implementation is relevant at all stages of design. The methodological solutions proposed in this article are focused on the initial stages of comparative evaluation of alternative structural solutions (without the need to use detailed technical data of the ship's systems, power plant, and ORC nodes), expected indicators of energy efficiency, and cycle performance. The development is based on generalized results of variation studies of the ORC in the structure of the widely used main marine medium-speed diesel engine Wärtsilä 12V46F (14,400 kW, 500 min^{-1}) in the operational load cycle range of 25–100% of nominal power. The algorithm of the proposed solutions is based on the established interrelationship of the components of the ORC energy balance in the P-h diagram field of thermodynamic indicators of the cycle working fluid (R134a was used). The implemented strategy does allow, in graphical form, for justifying the choice of working fluid and evaluating the energy performance and efficiency of alternative WHR sources for the main engine, taking into account the design solutions of the power turbine and the technological constraints of the ORC condensation system. The verification of the developed methodological solutions is served by the results of comprehensive variation studies of the ORC performed by the authors using the professionally oriented thermoengineering tool "Thermoflow" and the specification data of Wärtsilä 12V46F with an achieved increase in energy efficiency indicators by 21.4–7%.

Keywords: ship decarbonization; waste heat recovery; ORC; energy efficiency; structural formation algorithm

check for updates

Citation: Lebedevas, S.; Čepaitis, T. Methodological Solutions for Predicting Energy Efficiency of Organic Rankine Cycle Waste Heat Recovery Systems Considering Technological Constraints. *J. Mar. Sci. Eng.* **2024**, *12*, 1303. https://doi.org/10.3390/jmse12081303

Academic Editor: Leszek Chybowski

Received: 11 June 2024
Revised: 28 July 2024
Accepted: 29 July 2024
Published: 1 August 2024

1. Introduction

Decarbonization aimed at reducing greenhouse gas emissions (GHGs) is one of the highest priority tasks for maritime transport, considering its strong dependence on oil fuels mainly used in the engines of operating ships [1]. The rules, detailed in Annex VI to MARPOL 73/78 [2], are primarily aimed at decarbonization through improving the energy efficiency of ships. Thus, MARPOL Annex VI chapter 4 sets requirements for reducing

GHG emissions for newly built ships based on the regulated dynamics of changes in the energy efficiency design index (EEDI) [3]. From 1 January 2023, requirements for the introduced energy efficiency index for operating ships (EEXI) and the carbon intensity indicator (CII) came into effect. It is noteworthy that the initial International Maritime Organization (IMO) decarbonization strategy was fundamentally changed in 2018 with a commitment to achieve CO_2 emission neutrality by 2050, with a gradual reduction of emissions by 40% by 2030 and at least 70% by 2040 [1]. The normative documents of the European Union (EU) Parliament commission (COM) (2021)562 and 2021/0211/COD primarily link the decarbonization of maritime transport with the replacement of oil-based fuels used in ship power plants with renewable and low-carbon fuels (LCA): liquefied natural gas (LNG), biodiesel, methanol, ammonia, and hydrogen [4,5]. However, according to Det Norske Veritas (DNV GL) for 2023, only 6.5% of the gross tonnage (GT) of operating ships use renewable and LCA (LNG, biodiesel, methanol, and ammonia), and the share of these fuels among newly built ships is just over 50% [6].

The expected dynamics of decarbonization based on LCA [7] and in accordance with the strategic plans of IMO [1] indicate that in the mid-term perspective, up to 2030–2035, technological solutions will remain the priority tool for reducing GHG emissions (with a share of 15–35% in the overall balance). The strategic goal of decarbonizing maritime transport—"zero emissions" by 2050, according to DNV GL forecasts [6]—is expected to be achieved mainly through LCA, with twice the effect compared to technological solutions.

In the structure of technological solutions IMO [7,8], one of the directions with the greatest potential for decarbonization is the technology for utilizing secondary heat sources from the ship's power plant with a waste heat recovery system (WHR) [6]. According to DNV GL forecasts, improving the energy performance of ship power plants using WHR systems, with a theoretical potential of 50%, is estimated to range from 5 to 25% [6,9].

A significant amount of recoverable heat increases the attractiveness of WHR systems for marine applications [10]. At the same time, a review of information sources on the marine application of WHR indicates varying degrees of readiness of WHR technologies for practical implementation. In particular, technologies, such as thermal energy storage, hybrid cooling systems, Kalina cycles, adsorption desalination, and cooling systems, are still in the research stage [11].

The use of thermodynamic cycles, such as the Rankine Cycle or the Organic Rankine Cycle (ORC), are among other technologies in this field. Steam Rankine Cycles are not only adequately adapted and widely applied in WHR systems on marine vessels, but they are also already losing their effectiveness when used in modern power plants with advanced energy performance levels. At earlier stages of WHR application in shipping [11], high-temperature heat from sources like exhaust gases was used to evaporate the working fluid (usually water) in a boiler and produce steam to drive a turbine generator for electricity generation as well as steam for the heavy fuel heating system and the vessel's domestic needs. The increase in energy efficiency of modern engines reduces the energy potential of the Rankine Cycle using water steam, making Organic Rankine Cycles more relevant and prioritized for application.

ORC offers numerous advantages for waste heat recovery on ships compared to the steam Rankine Cycle. ORC systems use organic fluids with lower boiling points, enabling efficient operation at reduced temperatures. This is especially beneficial for modern marine diesel engines, as their exhaust gas temperatures tend to decrease with increased efficiency, making steam generation difficult due to the need for high-temperature heat sources. Such flexibility allows ORC systems to capture waste heat from a wider range of sources, including high-temperature and low-temperature WHR sources and auxiliary systems on ships [12].

Traditionally, high-temperature WHR sources include the energy potential of the exhaust gas system, which reaches 325–345 °C at nominal load for two-stroke engines and 360–380 °C for four-stroke engines. The temperature of the coolant in the engine cylinder cooling system, considered a low-temperature WHR source, typically ranges from

80 to 90 °C for most engines, although in some dual-fuel and gas engines, the cylinder head cooling water temperature can reach 125 °C [13]. The energy potential of this system, together with the lubrication system, is estimated at 8–10% of the external thermal balance. Additionally, modern marine engines with increased mean effective pressure also have significant WHR potential from the charge air cooling system, estimated at 14–17% of the engine's external thermal balance. The temperature range of the cooled supercharged air within the engine's operational load range of 100–250 °C makes it a very suitable candidate for WHR systems.

Primarily, the potential for implementing low-temperature WHR, constituting approximately 50% of the total WHR balance [14], makes the ORC (Organic Rankine Cycle) attractive for onboard use on ships. Additionally, organic fluids used in ORC systems are typically non-toxic and non-flammable, enhancing safety and reducing environmental risks. ORC systems are also more compact and lighter than steam cycles, simplifying their integration into existing ship designs [15,16].

It should be noted that besides the Organic Rankine Cycle, other cycles, such as the Brayton and Kalina cycles, are also used. The Kalina cycle is a modified version of the Rankine Cycle using a mixture of two liquids, usually water and ammonia, as the working fluid. However, the ORC is preferred in marine applications due to its greater flexibility, safety, lower maintenance requirements, and increased thermal efficiency. The ORC enables effective WHR from low-temperature sources with a simple design that requires minimal maintenance [17–21].

Despite the attractiveness of the potential energy efficiency of WHR systems based on the ORC, they have not been properly adapted for maritime use due to the lack of sufficient statistical research and operational prototypes. From 2015 to 2018, only five ORC–WHR systems were installed on ships, demonstrating energy efficiency improvements ranging from 3% to 15% [22,23]. Recently, the possibilities for their application have slightly expanded. The range of energy efficiency improvements for 13 operational power units with WHR–ORC systems has expanded to 6–22% using various combinations of the three low- and high-temperature waste heat sources [22,23], reaching up to 26% in a specific case [22]. In this latter case, the 26% energy efficiency was achieved in studies by M. Casisi, P. Pinamonti, and M. Reini thanks to operating the engine in the cold sea due to condensation pressure decrease.

Existing studies are primarily focused on justifying the achieved energy performance levels of the ORC, which, under equal power consumption conditions of the power unit, contribute to fuel consumption reduction and directly impact decarbonization efficiency in its maritime application.

For example, Vaj and Gambarotta [24] achieved a 12% increase in the energy efficiency of a power unit using exhaust gas energy and engine cooling liquid with an ORC system applied to a stationary internal combustion engine. Teng et al. [25] investigated a supercritical reciprocating Rankine engine, which avoids using the high-cost evaporator and is more conducive to system packaging. It is demonstrated in a case study that up to 20% of waste heat from the heavy-duty diesel engine may be recovered by the supercritical ORC–WHR system, making the efficiency for the hybrid energy system $\geq$ 50%. Casisi et al. [22] evaluated the option of recovering energy from an internal combustion engine for ship propulsion using a bottom ORC. In the study, a dual-fuel engine (six cylinders in line) with a power output of 5.7 [MW] and an efficiency of about 49% is considered for the ship's propulsion. Simulations revealed that a significant power gain (about 10%) can be achieved with the simple cycle. The use of the cooling water as a heat source might involve the use of an additional heat exchanger in order to avoid having too low return temperatures of the HT cooling water. According to the study, the regenerated ORC has the best compromise between performance and plant complexity. Grljusic et al. [26] evaluated a combined heat and power (CHP) system for an oil tanker using a supercritical ORC with working fluids R123 and R245fa, expanding the thermodynamic boundaries of the cycle and enhancing its energy performance. Their studies showed that CHP plant with R245fa fluid using supercritical ORC meets all of the demands for electrical energy and heat while burning only a small amount of additional fuel in auxiliary boiler. To enhance the cogeneration efficiency, the maximum temperature of the applied organic fluid should be increased to increase the turbine outlet temperature and improving the quality of the heat consumed on board. Song et al. [27] investigated the use of waste heat in an ORC system with a ship diesel engine rated at 996 kW and through the rational implementation of the ORC, achieving an increase in power station efficiency by 10.2%. ORC–WHR systems on ships, as demonstrated by Song et al. [27], also showed a fuel cost reduction ranging from 4% to 15%. The authors attribute the increase in ORC energy efficiency in their studies to addressing insufficiently studied aspects of onboard ORC application: rational combinations of WHR sources within the ORC structure, the structure of the WHR–ORC system itself, external thermal balance indicators under power unit operational conditions, the impact of hydrometeorological conditions (seawater temperature), and technical constraints imposed by ship systems, among others.

In Pantano et al. [28], a preliminary design of the considered expanders is proposed using custom models developed in MATLAB. The technical constraints specific to each machine are listed to facilitate the optimal selection of the expander based on efficiency, reliability, and power density. The final choice focused on the screw motor, for it is the 601 optimal compromise in terms of efficiency, lubrication, and reliability. In Ouyang et al.'s [29] parametric study of the dual-pressure organic Rankine Cycle system, six commonly used working fluids were assessed. Using the evaluation method's indicators as the objective function, the multi-objective optimization method was applied to determine the optimal operating conditions for the system.

Ng's study [30] and Casisi et al. [22] explored the detailed application of ORC systems in maritime transport, while Park et al. [31] provided a comprehensive review focusing on experimental ORC performance and conclude that ORC's conversion efficiency is not a function of the difference between heat source and heat sink temperatures but rather is related to evaporator and condensation temperatures. It has been concluded that ORC technology requires further research and development. Baldi et al. [32] analyzed a crucial aspect of WHR applicability on ships, focusing on how the operational load of marine power units affects the performance of WHR–ORC systems, and highlighting the significant role of this research direction across various types of vessels. Konur et al. [33] developed a thermodynamic model of an ORC system for diesel generators on tankers. Modeling results indicated a potential 15% reduction in fuel consumption of auxiliary engines and a 5.2% decrease in overall fuel consumption for the vessel. Akman et al. [34] conducted research showing that the waste heat from exhaust gases of two-stroke marine diesel engines possesses significant energy potential due to its high temperature. This makes it feasible to implement an ORC–WHR system operating in the supercritical region with a suitable working fluid. Their optimization study recommends that the power generation system integrated with ORC–WHR ideally operate in the range of 70% to 75% of the main engine's maximum continuous rating (MCR) to maximize exergy efficiency and minimize fuel oil consumption. Operating the ORC system under optimal conditions could potentially increase the efficiency of the power generation system by 2.53% [34].

An important aspect of WHR–ORC system research aboard ships is associated with assessing the impact of changing environmental conditions and the load cycle structure of the power unit, including variable loads, leading to the redistribution of WHR source potentials. In this regard, Ng introduced a new approach in his study [35] to evaluate the influence of exhaust gas heat profile characteristics using a standard operational scenario and an adapted model of exhaust gas heat for diesel engines, deemed a significant advancement in ORC onboard application design methodologies. Ng conducted a comparative analysis of two cycle configurations, basic ORC and recuperative ORC, demonstrating that recuperative ORC provides 16% higher net power compared to simple ORC. Tsui et al. proposed a more complex waste heat recovery system for diesel engines, incorporating a power turbine–SRC module and an ORC module. At full load, the total power generation reached 1079.1 kW, with the SRC–ORC module achieving maximum thermal efficiency and exergy efficiency of 28.5% and 65.7%, respectively, at 90% load [36]. The selection and justification of a rational combination of low-temperature secondary heat sources in complex WHR–ORC recovery systems are considered [37–41].

Grljusic et al. [42] implemented an ORC system driven by waste heat extracted from the exhaust gas, cylinder liner cooling water, and scavenge air of an oil tanker's main engine to generate power, and they saw an increase in the overall energy efficiency of the ship's power plant by more than 5% when the main engine operated at 65% or more of its specified maximum continuous rating. Sung and Kim [43] utilized waste heat from the exhaust gas and cylinder liner cooling water of a dual-fuel main engine on an LNG vessel for an ORC system. Their study revealed that the ORC system could produce a net output power equivalent to 5.17% of the main engine's power. Luo et al. [44] developed three variants of ORC systems designed to capture waste heat from exhaust gases and jacket cooling water of a marine medium-speed diesel engine and performed a comparative analysis of their energy performance indicators. Using the independent dual-cycle ORC system to recover the waste heat of ship diesel engine exhaust gas and jacket cooling water simultaneously results in the maximum output being 2.84% higher than that of the ORC system with a preheater. Shu et al. [45] introduced a thermal–economic evaluation model based on the operational profile to assess the utilization of the ORC for harnessing waste heat from marine engines. Their findings underscored the significant impact of operational conditions on the system's thermodynamic performance, indicating that both the peak thermal efficiency and net power output decrease as the engine load decreases, while, at the same time, the efficiency indicators of the ORC increase. Liu evaluated [39] a WHR system based on combination of the steam SRC and ORC using exhaust gas and jacket cooling water heat from a MAN B&W e14K98 marine engine. Their study showed a potential enhancement in engine thermal efficiency by 4.4% and a decrease in annual fuel consumption by 9322 tons at full engine load.

In terms of functional performance indicators, notable discoveries have been made regarding the implementation results of the ORC in the project of the vessel "Arnold Maersk", which utilizes heat from the engine's internal circuit. Although only one WHR source was used in the WHR–ORC system, several operational issues were identified. In particular, discrepancies in regulating the flow rate of the working fluid were observed, especially during reductions in seawater temperature [46]. The findings underscored the importance of aligning the specified characteristics of WHR–ORC with external operating conditions of the vessel and the operational modes of the engine. Among significant positive factors, a reduction in the weight of the entire ship's power unit by 12 tons could be achieved by replacing three auxiliary engine generators with a unified WHR–ORC system, along with a daily fuel consumption reduction of 2.1 tons [47]. Alternative WHR systems were also considered, where supercritical cycles are often used to capture high-potential waste heat, complementing the role of the ORC in recovering low-potential heat [41,47,48].

Pesyridis conducted a study [49] on a WHR–ORC system modeled for a marine diesel engine. The authors developed a MATLAB-based expander design code for calculating various expander geometrical characteristics. Additionally, they conducted an off-design study under different engine operating conditions. The results highlighted that the thermal efficiency of the cycle is significantly influenced by the engine's operating parameters. At higher engine speeds, the cycle demonstrated enhanced performance due to increased energy content and greater fluid evaporation. The impact of the WHR system on the engine's BSFC has been noted to decrease by 2.9–5.1% depending on operating conditions. It was found that the performance of the ORC system largely depends on selected regeneration circuit parameters, such as the mass flow rate of the working fluid, the available heat, and the heat exchanger efficiency. There was a trend towards increased useful power when higher refrigerant mass flow rates were used in the system. Similarly, ORC efficiency improved with increased coolant flow rates due to reduced condensation pressure. However, achieving optimal cycle performance requires careful consideration of limitations associated with adjusting ORC scheme parameters [49].

To expand the scope of the research, given the limited number of physical prototypes of WHR–ORC systems, the relevance of mathematical modeling methods is increasing. However, open-access analytical assessments of energy-efficient applications of WHR systems on ships and corresponding modeling are quite limited. In the computational study by Elkafas, waste heat from a two-stroke marine diesel engine installed on a container ship is considered for analyzing the performance of a new integrated WHR system involving the ORC and a thermoelectric generator (TEG). The study evaluates the impact of varying the organic working fluid's vapor pressure on the energy efficiency metrics of the ORC, such as generated power, the waste heat recovery rate, and the overall energy efficiency of both TEG and ORC systems, as well as the combined system [50]. In analytical studies, Niknam et al. explored the technical and economic value and benefits of integrated WHR systems for marine applications, assessing the system-level approach and understanding and analyzing the recovery of onboard WHR. The study also presents insights into the impact, value, and interdependence of several concurrent WHR technologies, focusing on new WHR technologies and the pioneering technical–economic structure of Mixed Integer Linear Programming designed for modeling and optimizing WHR metrics onboard [51].

Ng developed a thermodynamic model using modeling and analysis of multi-domain system software Siemens Industry Software NV Simcenter Amesim 2019 to explore four potential cycle configurations and evaluate five hydrocarbon working fluids in a commercial off-the-shelf system simulation software. The study utilized the operational profile and machinery design of a multi-purpose platform service vessel (MPSV) operating in the offshore oil and gas industry in Southeast Asia as a case study to assess the feasibility of installing an ORC system onboard. The thermodynamic analysis results indicated that a net power output of approximately 160 kW could be achieved for a diesel engine with a rated output of 1950 kW, with ORC efficiencies ranging from 17% to 20%. The configurations using cyclopentane and methanol as working fluids, particularly the recuperated ORC (rORC) configuration, demonstrated promising performance [40]. In the research conducted by Duong et al. [52], an integrated gas turbine, ORC, and steam Rankine Cycle system utilizes LNG cold energy and waste heat from the system to convert it into useful work and power. The energy and exergy efficiencies of the proposed system were calculated to be 68.76% and 33.58%, respectively. The waste heat recovery combined cycles generated an additional 2100.42 kW, which is equivalent to 35.6% of the system's total output. This confirms that the combination of waste heat recovery and cold energy utilization systems is suitable for power generation and increasing systems' thermal efficiency.

Research and practical experience with waste heat recovery Organic Rankine Cycle (WHR–ORC) systems indicate that implementing these systems on ships is notably more complex than on land-based power plants. As many studies show, the complexity arises from the variability of secondary heat sources aboard ships, which fluctuate depending on load conditions, particularly within the operational load range specified in ISO 8178 [53]. Research on optimizing ORC systems at various load levels and the influence of seawater temperature has been limited, complicating practical assessments for decision making regarding the applicability of WHR–ORC. Most experimental and computational studies are focused on optimizing pre-configured structures of WHR–ORC systems. Such an approach during the initial decision-making and preliminary design phases hinders comparative exploratory assessments for selecting a rational recuperation scheme. Conducting similar assessments regarding expected energy system performance, particularly WHR–ORC recuperation systems in this application, should ideally be based on energy balance considerations, abstracting from specific model technological parameters. Considering the operational characteristics of onboard ORC applications, it is rational to combine assessments of the impact of the operational load cycle structure of the power plant, the seawater temperature, and possible ship technological systems involved in the ORC structure.

Currently, Klaipeda University is conducting extensive research on decarbonization strategies, with a particular focus on the rational application of ORC technology. Previous studies [54,55] have covered several key aspects of ORC application within ship power plants, including the evaluation of optimal working fluids for ORC systems (considering environmental constraints), individual and combined use of secondary heat sources in the operational load cycle of the main power unit, analysis of ships' technological constraints, and the formation and optimization of ORC structural configurations. Through comprehensive research, the university aims to identify the most effective ways to integrate ORC technology into various applications, considering various factors, such as environmental sustainability, energy efficiency, and practical feasibility. This study represents a continuation of previous research efforts and is viewed as a significant contribution to expanding the application area of the ORC in maritime transport.

The research conducted includes the following interconnected methodological tasks:

- Determining and analyzing the interrelationship of ORC energy balance components through structural analysis of the WHR cycle, alongside numerical variational studies.
- Justifying the principles of energy-efficient combined use of secondary heat sources (exhaust gases, cylinder cooling, compressed air cooling) in the ORC system, considering the operational load cycle according to ISO 8178 E3.
- Developing methodological foundations for forming a rational WHR configuration in the ORC cycle, considering ships' operational and technological constraints.

The content of the research is oriented towards applying the ORC in conjunction with the widely used four-stroke medium-speed main diesel engine "Wärtsilä" 12V46F in the fleet, with a working range of 25–100% of nominal power. At the stage of research presented in this publication, data on the interrelation of WHR cycle energy performance with seawater intake (which shapes the technological requirements for pumps in the WHR fluid condensation system), methodological considerations for selecting the WHR structure in the ORC cycle of ship power plants, ORC energy efficiency assessments, and defining rational cycle energy parameters considering constraints are provided.

2. Methodological Aspects of the Research

The research selected the "Wärtsilä" 12V46F four-stroke marine diesel engine because of its extensive engine series and wide nominal power (Pe) range. This engine design shares similarities with models offered by other leading marine diesel engine manufacturers, broadening the study's relevance (main parameters presented in Appendix B, Table A1). The operational cycle for the engine is tailored based on the type of ship it is installed in. For instance, ferry-type vessels operate under the E3 operational cycle, with main engine specifications adhering to ISO 8178 standards. An ORC–WHR simulation model was created using the thermo-engineering program "Thermoflow" (USA) (Appendix A) to analyze and evaluate the performance of this waste heat recovery cycle system.

This methodological section is a continuation of the one previously presented in the authors' publications [54,55], which describes the main methodological solutions of cycle parameters and their formation. The research involves conducting continuation analyses and formulating the theoretical alignment and optimization of the ORC structure and its energy indicators according to external and technological constraints characteristic of maritime transportation.

The methodological aspects of the Rankine Cycle in WHR systems in this study are based on the Organic Rankine Cycle energy balance, which is analyzed using the Mollier diagram, which graphically illustrates how changes in boundary conditions affect the thermodynamic properties of the working fluid throughout the entire cycle. Accordingly, based on readily available Mollier diagrams of working fluids and conducted simulation calculations using the "Thermoflow" software, a graphical evaluation and analysis of the WHR cycle were compiled.

The representation of the cycle calculation on the Mollier diagram is based on the p-h (pressure–enthalpy) form (see Figure 1).

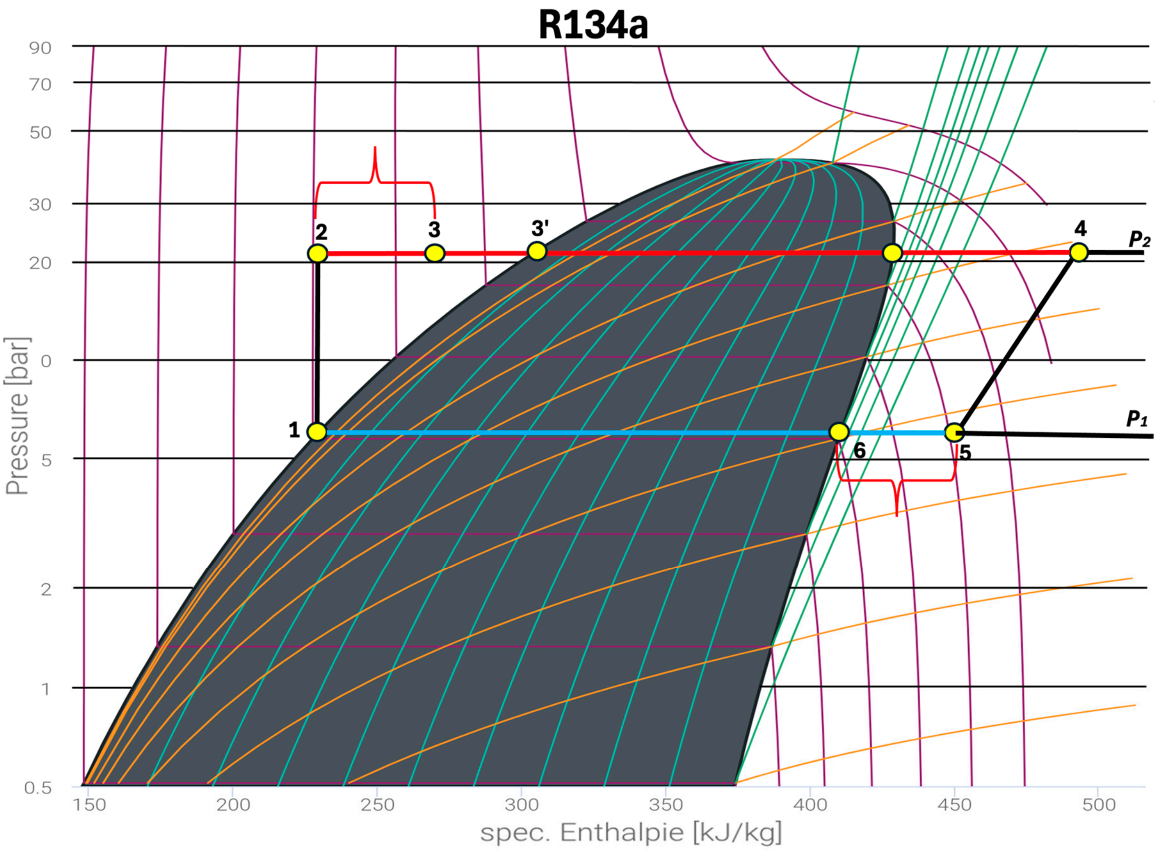

Figure 1. WHR cycle characteristic points representation in the working material Mollier chart.

The main condition is that the preliminary heating of the WF in the RHE may not reach the vaporization starting point or, conversely, transition into the vaporization region. Therefore, unlike the schematic in Figure 1, a more generalized version of the WHR cycle is analyzed. Emphasizing the variability of the preliminary heating process of the working fluid in the recuperative heat exchanger, the graphical analysis expands the evaluation of the WHR cycle under different implementation boundary conditions.

The thermal parameters at characteristic points of the cycle are determined in the following sequence:

- The position of line P_1 on the Mollier diagram is determined based on the chosen working fluid's condensation pressure at the near-bulk seawater temperature (t_w) in the condenser. The heat conversion from saturated vapor (Figure 1, Sections 5 and 6) to saturated liquid (Figure 1, Section 6.1) for the working fluid condensation is identified by calculating the heat transfer per unit mass of the working fluid, expressed in kJ/kg

$$(q_{condenser} = (h_6 - h_1)) \tag{1}$$

- The position of point P_2 for the working fluid is determined based on the specified pressure drop degree π_T in the turbine (Figure 1, Sections 4 and 5), which ensures the operation of the pump. Position 2 is identified on the diagram according to the condition $h_1 = h_2$;
- The heat transfer Q_{SS} from the engine heat source/sources (exhaust gases, cylinder cooling circuit, scavenge air cooling circuit) is calculated, which is converted into a specific form per 1 kg of working fluid, denoted as q_{ss} (based on the principle outlined in the Mollier diagram): $q_{ss} = \sigma h_{ss}$. Thus, the length of the segment 4-3 is identified based on enthalpy, without specifying the exact positions of 3 and 4 on the diagram;

- Positions 3 and 4 on the diagram are iteratively identified in the field, determining the initial value of heat transfer in the regeneration heat exchanger σh_{RHE}, which identifies position 5;
- The position of point 4 on line P_2 is calculated based on the change in the working fluid temperature during expansion in the turbine ($t_4 - t_5$).

$$T_5 = T_4 - T_4\left[1 - \frac{1}{\pi_T^{\frac{K-1}{K}}}\right]\cdot\eta_{T.ad.} = T_4\left[\frac{1}{\pi_T^{\frac{K-1}{K}}}\right]\cdot\eta_{T.ad.} \rightarrow T_4 = T_5\cdot\frac{\pi_T^{\frac{K-1}{K}}}{\eta_{T.ad.}} \quad (2)$$

where K—coefficient of the adiabatic expansion of the working fluid; $\eta_{T.ad.}$—projected adiabatic efficiency of the turbine; and π_T—degree of pressure reduction in the turbine for the working fluid (determined based on initial conditions);
- The alignment of position 4 on the diagram is evaluated using two methods: calculating from position 5 and determining the position as the sum of two segments on line P_2 in the diagram ($h_{RHE} + h_{ss}$). If the position determined using the two methods differs by $\geq 2\%$, the segment h_{RHE} is adjusted, and the alignment process is repeated until the error does not exceed the specified tolerance.

The algorithm for the formation of the WHR cycle structure and the determination of the sequence of parameters is compiled and presented in Figure 2 in the form of a block diagram.

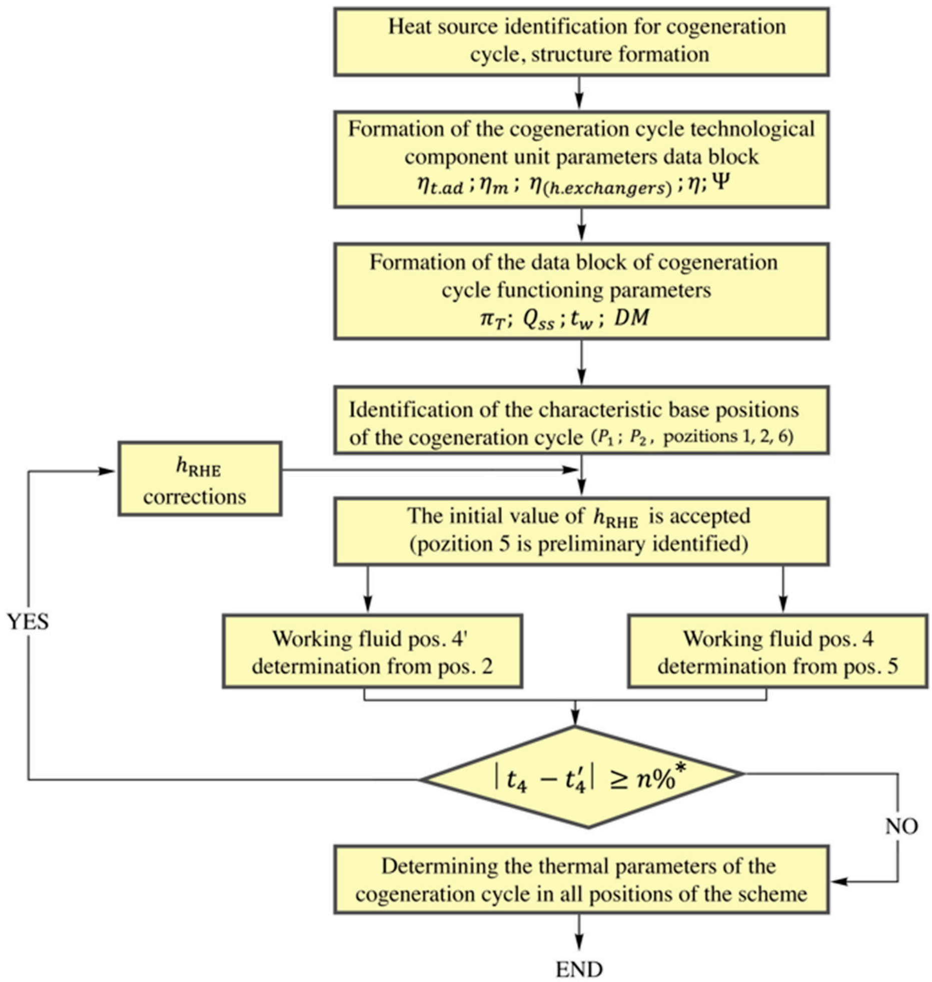

Figure 2. Algorithmic approach to constructing the WHR cycle configuration and parameter identification. * Error is determined by assessing the accuracy of the initial data of the methodology.

After forming the rational structure of the Rankine Cycle, considering technological constraints and hydrometeorological conditions (seawater temperature), its energy indicators and their impact on improving the energy efficiency parameters of the ship's power plant are determined based on the analytical solutions provided below.

Evaluation of η_{eR} for a power plant with an ORC where three diverse heat sources are present:

$$\eta_{eR} = \frac{(P_{turb} + P_e)}{H_u \cdot G_f} \tag{3}$$

where P_{turb} is formed from the (complex secondary heat sources case) supplied heat from the three secondary heat sources.

In the common secondary heat source case,

$$P_{turb} = Q_{\in}(\eta_{t.ad} \cdot \eta_m \cdot \Psi_{turb}) \tag{4}$$

where $Q_{\in}$ is the heat supplied to the turbine. Heat conversions also take place within the turbine, $\Psi_{t.cil} = \frac{h_{w1} - h_{w2}}{h_{w1} - h_w{}'}$, when $h_{w1} - h_{w2}$ is an actual decrease, and $h_{w1} - h_w{}'$ decrease that is required as per the specification.

The energy utilization factor for inflatable air is evaluated similarly.

$$q_{cil} = \frac{Q_{cil}}{H_u \cdot G_f} \tag{5}$$

$$q_{sc.air} = \frac{Q_{sc.air}}{H_u \cdot G_f} \tag{6}$$

$$Q_f = H_u \cdot G_f \tag{7}$$

As a result,

$$P_{turb} = ((Q_{exh} \cdot \eta_{h.exh} \cdot \Psi_{exh}) + (Q_{cil} \cdot \eta_{h.cil} \cdot \Psi_{cil}) + (Q_{sc.air} \cdot \eta_{h.sc.air} \cdot \Psi_{sc.air})) \cdot \eta_{t.ad} \cdot \eta_m \cdot \Psi_{turb}. \tag{8}$$

Therefore, the overall efficiency of the power plant utilizing the ORC–WHR cycle with three secondary heat sources is calculated using the formulas

$$\eta_{eR\in} = \frac{H_u \cdot G_f (q_{exh} \cdot \eta_{t.exh} \cdot \Psi_{t.exh} + q_{cil} \cdot \eta_{t.cil} \cdot \Psi_{t.cil} + q_{sc.air} \cdot \eta_{sc.air} \cdot \Psi_{sc.air}) \cdot (\eta_{t.ad} \cdot \eta_m \cdot \Psi_{turb})}{H_u \cdot G_f (q_{exh} + q_{cil} + q_{sc.air})} \tag{9}$$

Coefficient η_{eR} of the main engine increased with the WHR system cycle:

$$\sigma\eta_{eR} = \frac{(q_{exh} \cdot \eta_{t.exh} \cdot \psi_{t.exh} + q_{cil} \cdot \eta_{t.cil} \cdot \psi_{t.cil} + q_{sc.air} \cdot \eta_{sc.air} \cdot \psi_{sc.air}) \cdot (\eta_{t.ad} \cdot \eta_m \cdot \Psi_{turb})}{\eta_e}.$$

The alternative method for determining P_{turb} aims to identify and enhance the factors affecting the efficiency of the WHR cycle. This approach allows for optimizing the operational parameters of the cycle's power turbine and establishing their correlation with a rational selection.

The power produced in a propulsion turbine is described by the equation

$$P_{turb} = G_{wm}(h_{tg_1} - h_{tg_2}) \tag{10}$$

ORC efficiency is determined by Equation (11):

$$\eta_{RC} = \frac{H_u \cdot G_f (q_{exh} \cdot \eta_{t.exh} \cdot \Psi_{t.exh} + q_{cil} \cdot \eta_{t.cil} \cdot \Psi_{t.cil} + q_{sc.air} \cdot \eta_{sc.air} \cdot \Psi_{sc.air}) \cdot (\eta_{t.ad} \cdot \eta_m \cdot \Psi_{turb})}{H_u \cdot G_f (q_{exh} + q_{cil} + q_{sc.air})} \tag{11}$$

WHR cycle efficiency, η_{RC}, determines how efficiently the secondary heat sources are transformed into the turbine mechanical work and further converted into electricity in the generator.

The design of the turbine nozzle apparatus is characterized by the parameter π_T, which indicates the extent of pressure reduction of the working medium before and after the turbine. The power generated in the turbogenerator is also represented by the Equation (12):

$$P_{turb} = G_{wm} \cdot t_{wm_1} \cdot c_{p_{wm}} [1 - \pi_T{}^{\frac{K-1}{K}}] \cdot \eta_{t.ad} \cdot \eta_m \cdot \beta \quad (12)$$

β—energy input impulse coefficient, which is 1.0 under WHR cycle conditions.

k—adiabatic indicator.

Describing P_{turb} in two distinct forms is advantageous. By optimizing the operational parameters of the turbogenerator and understanding their relationship with optimal choices, we can identify and enhance factors that impact the efficiency of the WHR cycle. This evaluation assesses the efficiency η_{RC} of the WHR cycle, measuring how effectively secondary heat sources are converted into mechanical work in the turbine and subsequently into electricity by the generator.

3. Methodological Solutions for Selecting Rankine Cycle Applicability Indicators in the Ship's WHR System

Based on the analysis of performed variational studies [54,55], a number of methodological solutions have been formulated for assessing the energy performance indicators of the ORC cycle, justifying the rational structure, and coordinating the operation within the ship's power plant at the preliminary stage of decision making in the regeneration of secondary energy sources (results presented in Appendix B, Tables A3 and A4). The methodology aims to develop tools for conducting a comparative assessment and justifying rational decisions for choosing alternative WHR–ORC structure options, with the implementation of an assessment of the expected energy efficiency indicators of the cycle in the ship's power plant, under specific operational and technological conditions. The interrelation of the proposed methodological solutions includes the following components (to avoid duplication, the solutions presented below are summarized with references to the authors' publications, which provide a detailed explanation).

3.1. Variable Evaluations of Energy Performance of the Cogeneration Cycle

3.1.1. Determining the Limit Functioning Conditions of the ORC Cycle Based on Energy Performance Indicators of the Main Power Plant and the Expected Meteorological Water Environment of the Ship's Operating Area

- The heat balance data of the manufacturer's main engine specifications are supplemented using classical analytical solutions in the theory of internal combustion engines (for operating cycle with load modes of 100–25% of the main engine's nominal power) (see Appendix B, Table A2).
- The temperature of the seawater (overboard water) t_w and its possible variation range are evaluated.

3.1.2. Description of the Possible Structural Parameters of the ORC Cycle

- Based on the heat balance data of the ship's power plant, the energy potential of secondary heat sources is determined, and the rationality of their individual or combined use in the WHR–ORC structure is assessed.
- The design of the power turbine for ORC is selected for WHR regeneration within the operating cycle load range (a turbine with a variable nozzle geometry implementing $\pi_T = const$ or $\pi_T = var$ i under characteristic engine load conditions and the corresponding variable range of the ORC working fluid flow).
- Based on the research results [54], the most suitable working fluid for use in the cycle is identified according to energy efficiency indicators and performance. In the absence of data from previous studies, the selection of the working fluid according to energy

efficiency indicators is carried out based on the sequentially performed stages of WHR–ORC formation described below in the Mollier diagram environment.

- In parallel with the energy performance indicators, the saturation pressure of the working fluid at the t_w level is evaluated to achieve the minimum possible pressure of the working fluid after condensation from the standpoint of the reliability of the WHR–ORC design under equal conditions. As a result, the working fluid pressure P_1 is determined and plotted on the Mole diagram. Equally important is the evaluation of the working fluid according to current and prospective environmental regulations. For example, in the conducted studies, R134a was chosen as the working fluid. According to the revised EU Regulation 517/2014 [56], from 1 January 2025 (with various exceptions until 1 January 2026), the use of fluorinated GHG with a GWP of 2500 or more for servicing and repairing all refrigeration equipment is prohibited. However, this ban will not apply until 1 January 2032, to regenerated fluorinated GHG with a GWP of 2500 or more, used for technical servicing or repair of existing air conditioning and heating equipment. From 1 January 2032, the use of fluorinated GHG with a GWP of 750 or more (up to 2500) is prohibited, except for regenerated fluorinated GHG used in the repair and maintenance of refrigeration equipment. Thus, in EU ports and after 1 January 2032, for existing installations with a refrigerant having a GWP of no more than 2500, replenishment is possible solely through a regenerated or recycled product. Among HCFCs with a GWP below 2500, for the most part, the single-component refrigerant R134A and the blend R407F are used on ships with the class Register [54,55]. Based on this, taking into account the EU regulatory restrictions, as well as the results of the authors' first phase of research, freon R134a with an ozone depletion potential of 1430 [54] was used for further research.
- Energy efficiency parameters of heat regenerator units are defined: η_{ti}, Ψ_i, $\eta_{T.ad.}$, $\eta_{T.m.}$ (described in [54,55]).

3.1.3. Evaluation of the Regulation of the Variable ($\boldsymbol{\pi_T = var}$), the Operation, and the Mechanical Power Output of the Turbo Generator's Power Turbine

Variational evaluations of the WHR–ORC cycle ($\pi_T = var$) regulation, functioning, and generated power in the power turbine generator P_{turb} are performed in the field of the Mollier diagram of the selected type of the working fluid, where the graphic dependence $P_{turb} = f(G_w, \pi_T = var)$ is formed (Figure 3).

- The evaluated working fluid is identified by the P_1 level in the Mollier diagram according to the seawater temperature t_w. Characteristic points 6 and 1 are formed in the diagram (the start and the end of condensation of the working fluid in the condenser);
- For the alternatively selected variation sequence evaluated for implementation in the cycle π_T; $\pi_T{}'$; $\pi_T{}''$; $\pi_T{}'''$, pressure point $P_2{}'$; $P_2{}''$; $P_2{}'''$ values are identified and represented in the Mollier diagram field;
- Based on the functioning principles of the recuperative heat exchanger, with condenser interface, variable working fluid enthalpy sections $\left(h_3{}' - h_2{}'\right)$, $\left(h_3{}'' - h_2{}''\right)$, $\left(h_3{}''' - h_2{}'''\right)$ are repeated in the form of $\left(h_6 - h_5{}'\right)$, $\left(h_6 - h_5{}''\right)$, $\left(h_6 - h_5{}'''\right)$ in the P_2 horizontal line;
- For each $t_5{}'$; $t_5{}''$; $t_5{}'''$ temperature value according to Equation (2), temperature values $t_4{}'$; $t_4{}''$; $t_4{}'''$ are calculated, corresponding to the temperature of the working fluid at the turbine inlet; therefore, positions of the working fluid state are identified in the P_1 horizontal line in the form of 4/, $4''$, $4'''$.

As a result, the energy scheme of the WHR cycle in the field of the Mollier diagram is developed; it is the basis for evaluating energy performance, efficiency, and condensation functioning of the optimal WHR cycle.

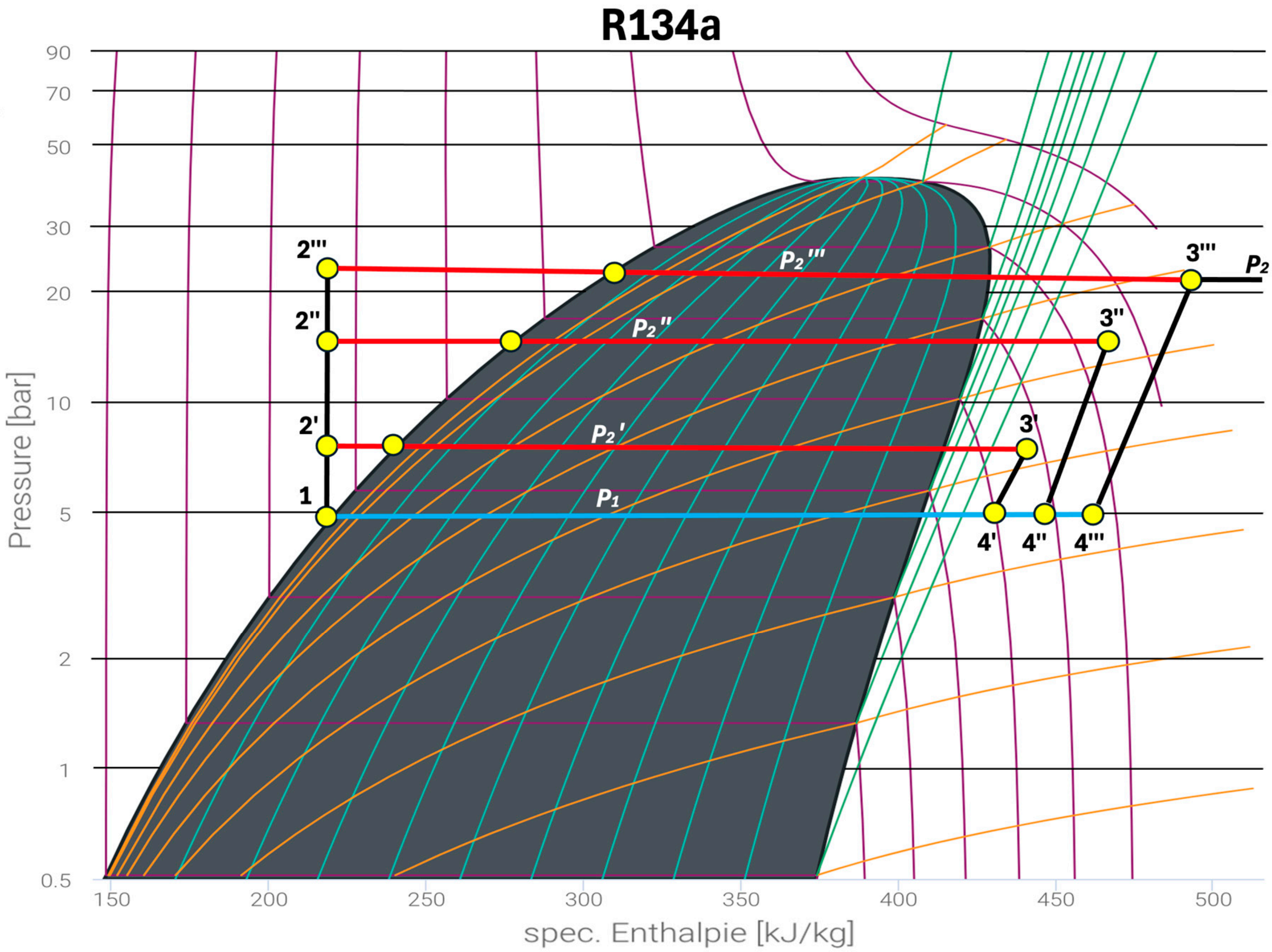

Figure 3. Variational estimation scheme of $P_{turb} = f(G_w, \pi_T = var)$ represented in the Mollier diagram $\left(\pi_T{}' = \frac{P_2{}'}{P_1};\ \pi_T{}'' = \frac{P_2{}''}{P_1};\ \pi_T{}''' = \frac{P_2{}'''}{P_1}\right)$.

3.2. Optimization Evaluations of Energy Performance of the WHR Cycle

3.2.1. Determination of the ORC-Generated Mechanical P_{turb} Energy

The WHR–ORC-generated mechanical energy P_{turb} is determined by referring to the data of the selected WHR–ORC heat sources Q_{SS} of the main engine:

$$P_{turb} = \left[\sum_{i=1}^{n} Q_{ss_i} \cdot \eta_{t_i} \cdot \Psi_i\right] \cdot \eta_{T.ad.} \cdot \eta_{T.m.}. \tag{13}$$

3.2.2. Variable Evaluation of the Flow Rate of the Working Fluid

The flow rate of the working fluid in variational estimates is equal to

$$G_{WF} = \frac{\left[\left(\sum_{i=1}^{n} Q_{ss_i} \cdot \eta_{t_i} \cdot \Psi_i\right)\right]}{(h_4 - h_3) - invar}. \tag{14}$$

3.2.3. Variational Evaluation of the Ship's Water Intake Pump Performance

The variational evaluation of the flow rate of the seawater pump is the following:

$$G_w = \frac{\left[\left(\sum_{i=1}^{n} Q_{SS_i} \cdot \eta_{t_i} \cdot \Psi_i\right) - P_{turb}\right]}{h_6 - h_1} \tag{15}$$

3.3. Graphical Methods for Optimizing ORC Parameters

3.3.1. Graphical form for Determining the Interdependence Parameters of P_{turb} and G_w Considering the Technological Constraints of the Condensation System

According to the obtained data on P_{turb} and G_w, when $\pi_T = var$, the correlations between the graphical form of the parameter optimization and rational values of the cycle are developed.

3.3.2. Selection of the Operational Indicators of the ORC Cycle for Rational Energy Functioning

The following tasks are addressed in the selection of rational energy parameters for the ORC:

- Determining the energy performance of the WHR cycle considering the technological constraints of the ship's water intake pump of the condensation unit.
- Comparative assessment of the energy indicators of heat regeneration from the mechanical power of the power turbine in the range of partial load modes of the main engine for the rational selection of the design ($\pi_T = const$ or $\pi_T = var$).

3.3.3. Graphical Representation of the Relationship between $\boldsymbol{P_{turb}}$ and $\boldsymbol{G_w}$ Parameters

According to the solutions in the methodology, the results of earlier studies [55] are summarized in graphical form, depicting the relationship between P_{turb} and G_w parameters in graphical form (Figure 4).

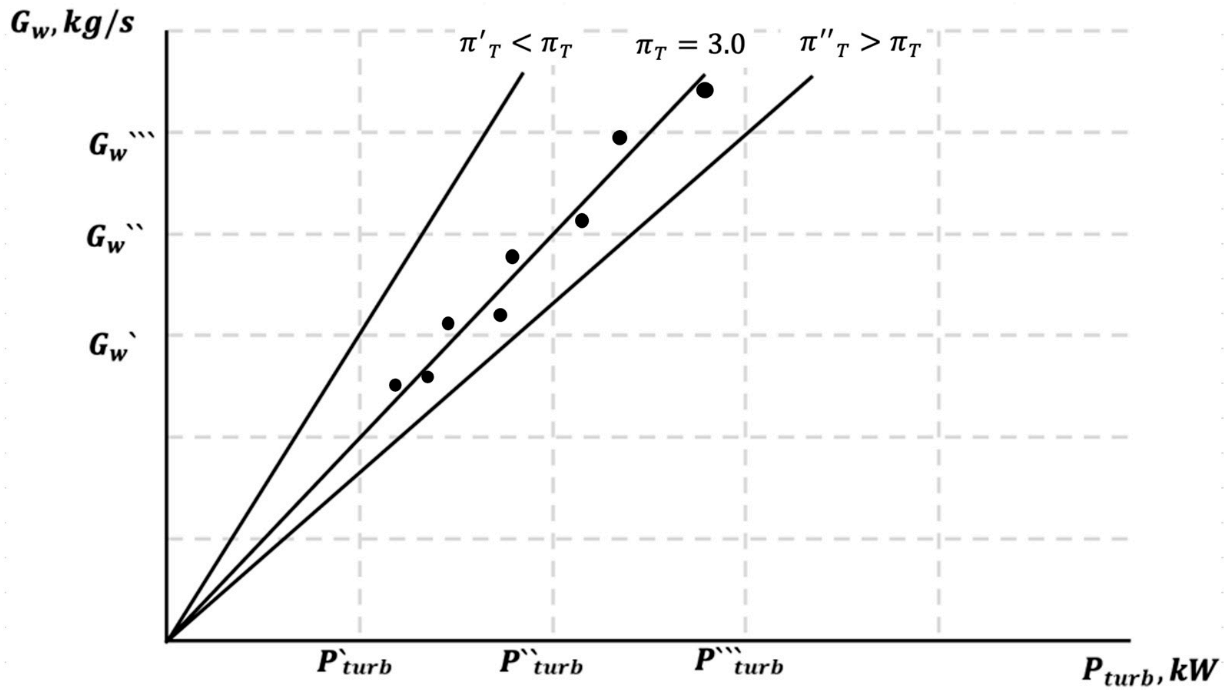

Figure 4. Graphical dependence of the parameters of P_{turb} and G_w on $\pi_T = var$.

According to the previously presented analytical justifications of [55] $\frac{G_w}{Q_T} = const$, when $\pi_T = const$, each of the lines in the P_{turb} and G_w interrelation describes the entire range of possible options for incorporating the heat sources in the WHR–ORC cycle when a power plant is operating in a wide range of load modes (see Figure 5).

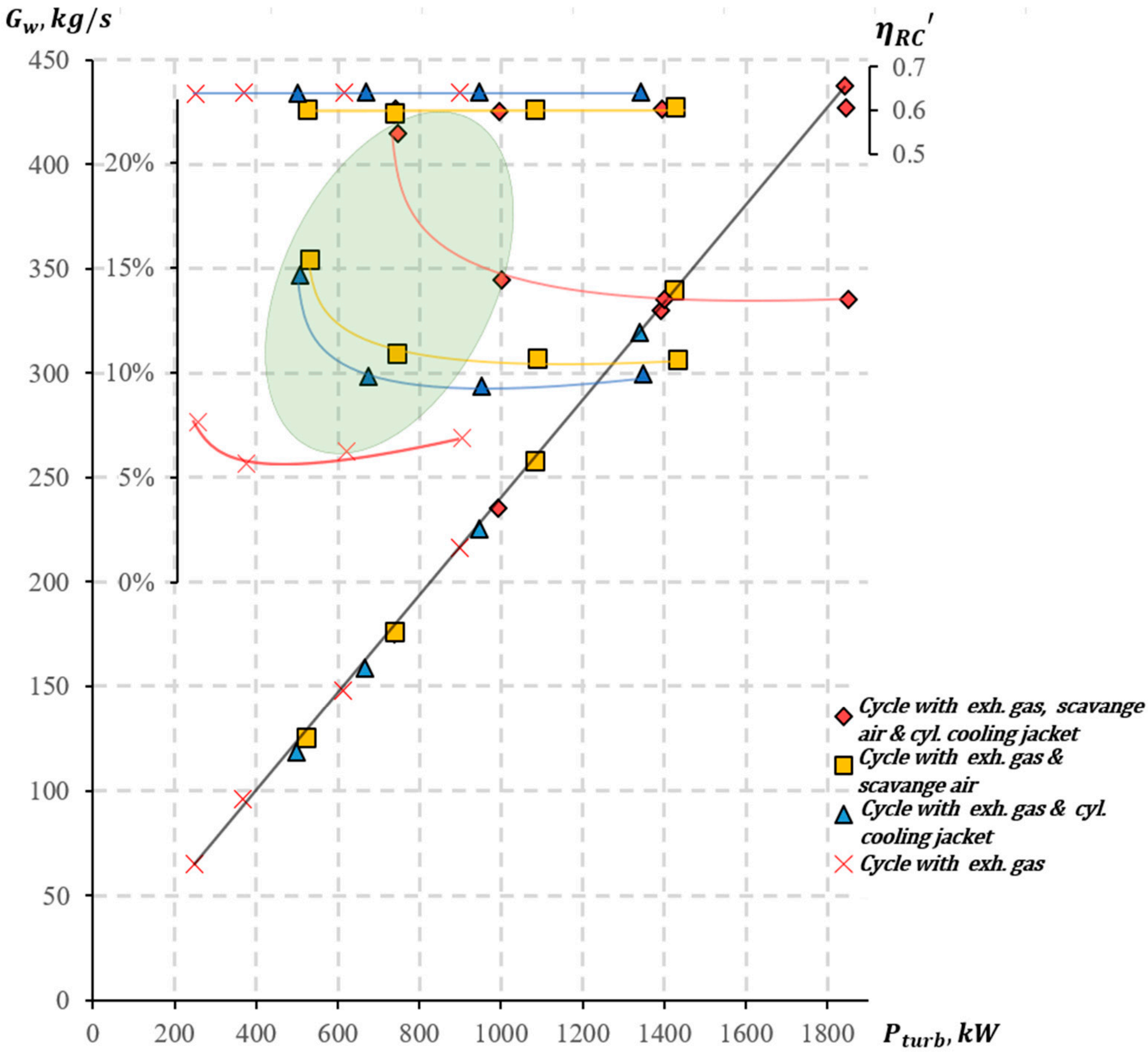

Figure 5. The interrelation of the P_{turb} and G_w parameters with the variants of incorporating possible secondary heat sources in the WHR cycle in a wide load range.

3.3.4. Identification of the Compression Ratio of the Power Turbine $\pi_T = var$ at Partial Load Modes of the Main Engine

After implementing methodological decisions Sections 3.2 and 3.3, the same conditions can be applied to the design variant of the turbine with $\pi_T = var$ and a fixed nozzle apparatus.

The values of the turbine expansion ratio π_T in partial load modes are determined according to the turbine specification characteristics $\pi_T = f(G_{WFi}, t_i)$, then they are identified in the field of $P_{turb} = f(G_{wi}, \pi_T = invar)$ in Figure 3.

Finally, specific energy performance indicators of the WHR cycle are forecasted for the turbine model in operational load modes of the main engine. Additionally, in the rational implementation of the WHR cycle, the range of operational loads is assessed to achieve a higher $\delta\eta_e$.

The transition to complex operational evaluations of ORC efficiency indicators $\delta\eta_e$, taking into account the structure of the operational load cycle of the main engine, is performed using the regulatory decisions of ISO 8178 (E3 or E2 depending on the design of the ship's propulsion system).

Thus, the methodological solutions developed based on conducted variational studies enable the selection and evaluation of expected ORC energy performance indicators using a convenient graphical representation for decision making. This representation depicts the relationship between ORC energy performance indicators and functional parameters of the main engine under its operational characteristics and conditions.

4. Conclusions

The results presented in the article are related to the application of the WHR–ORC systems of ship power plants. The aim and content of the research were to develop methodological solutions, evaluate energy efficiency, and produce rational utilization structures of WHR in WHR–ORC systems.

The originality of the proposed solutions lies in their focus on pre-project decision-making stages and does not assume a detailed design scheme of the WHR–ORC with results of analytical analysis of its parameters. The energy stability of the solutions is ensured through a combined analysis of the interrelationship of ORC energy balance components on the Mollier (P-h) diagram of the cycle working fluid. The analytical assessments of ORC energy performance are based on classical solutions of technical thermodynamics and turbomachinery theory. The evaluation includes assessing the impact of ship systems' technological constraints, such as the performance of condensation pump systems for the working fluid (G_w), seawater temperature in the ship's operating area, and limits of working fluid saturation (T-P), which restrict the upper potential of WHR energy plant realization.

It is indicative that the experimentally established and subsequently analytically justified stability of the G_w interrelationship with the energy performance of the power turbine generator serves as the basis for unified principles of comparative assessments under any configuration of secondary energy sources in ORC.

The chosen ORC analysis strategy allows for justifying the selection of the cycle working fluid through successive assessments of energy performance on the Mollier diagram.

The development is based on systematizing and analytically summarizing previous variation study results by the authors [54,55] on ORC configuration and energy performance in onboard applications with the medium-speed main engine Wärtsilä 12V46F (14,400 kW, 500 min^{-1}). These studies showed potential for increasing energy efficiency $\sigma\eta_{eRC} \approx$ 21.4–7.0% in the operational load range of 25–100% of the main power plant's nominal power. Using the engine manufacturer's specification data in conjunction with professionally oriented thermoengineering software (such as "Thermoflow", USA) allows for considering the results of these studies as verification of the methodological developments presented in this publication.

Further research should logically link the adaptation of proposed methodological developments to various ORC configurations and verification with the performance of implemented WHR–ORC system projects.

Author Contributions: Conceptualization, S.L.; methodology, S.L.; software, T.Č.; validation, T.Č.; analysis, S.L. and T.Č.; investigation, S.L.; data curation, S.L. and T.Č.; writing—original draft preparation, S.L. and T.Č.; writing—review and editing, S.L. and T.Č.; visualization, T.Č.; funding acquisition, T.Č. All authors have read and agreed to the published version of the manuscript.

Funding: This research received no external funding.

Institutional Review Board Statement: Not applicable.

Informed Consent Statement: Not applicable.

Data Availability Statement: The original contributions presented in the study are included in the article, further inquiries can be directed to the corresponding author.

Acknowledgments: The authors are grateful to the developers of the thermal engineering software "Thermoflow" for the opportunity to run cycle simulations for the experimental research. The authors are grateful to the company "Thermoflow Inc." for the thermal engineering software "Thermoflow" and the possibility to run cycle simulations for the experimental research. Research was carried out according to plans of the Research Council of Lithuania and the Ministry of Education, Science and Sport Lithuania (Contract No. S-A-UEI-23-9).

Conflicts of Interest: The authors declare no conflicts of interest as the parametric analysis is the authors' decision.

Nomenclature

G_{air}	charge air flow before entering the engine cylinder, kg/s
$\mathrm{G_{WF}}$	flow rate of working fluid, kg/s
$\mathrm{G_f}$	hourly engine fuel consumption, kg/s
G_w	seawater flow rate, kg/h
$\mathrm{H_u}$	lower fuel calorific value, kJ/kg
h_{w1}; h_{w2}	enthalpy of the working fluid before and after cylinder cooling jacker heat exchanger, kJ/kg
$h_w{}'$	enthalpy value, which is necessary according the engine manufacturer's specification, kJ/kg
k	specific heat ratio
K_1	the cumulative efficiency of the power turbine
P_e	main engine power, kW
P_{turb}	the power generated by the turbogenerator of the WHR system, kW
t_w	seawater temperature, °C
t_{WF_1}	temperature of the working fluid, °C
$\mathrm{Q}_{exh.}$	power plant exhaust gas energy part of heat balance, kJ/s
Q_f	total fuel energy, kW
$Q_{sc.air}$	power plant scavenge air cooling energy part of heat balance, kJ/s
Q_{oil}	power plant lubricating oil cooling energy part of heat balance, kJ/s
$\mathrm{Q_{cil.}}$	power plant cylinder cooling jacket energy part of heat balance, kJ/s
$\mathrm{Q_w}$	WHR cycle heat dissipation through overboard water, kJ/s
Q_h	total heat transferred per unit mass of working fluid, kJ/s
Q_{SS}	secondary heat source transferred heat, kJ/s
Q_T	transformed heat in the turbine into mechanical work, kJ/s
$q_{exh.}$; $q_{cil.}$; $q_{sc.air}$	specific heat of secondary heat sources, kJ/kg
q_h	heat transferred from the working substance to the condenser, kJ/kg
q_{SS}	transferred specific heat from secondary heat sources to WF, kJ/kg
π_T	the degree of pressure drop in the turbine
η_e	coefficient of performance of the main power plant
η_eRC	the total coefficient of performance of the ship's main power plant with a WHR system
η_{RC}	coefficient of performance of the WHR cycle
$\delta\eta_{eRC}$	relative change of ship power plant efficiency with and without ORC
$\eta_{eRC_{cikl}}$	ship power plant efficiency with ORC with ISO 8178 operational cycle
$\eta_\mathrm{t.sc.air}$; $\eta_\mathrm{t.cil.}$; $\eta_\mathrm{t.exh.}$	thermal efficiency coefficient of the secondary heat source exchangers
$\eta_{t.ad}$	internal (adiabatic) efficiency of the turbogenerator
η_{ti}	thermal efficiency of the secondary heat sources' heat exchanger
η_m	mechanical efficiency of the turbogenerator
$\Psi_{t.cil}$; $\Psi_{t.sc.air}$; $\Psi_{t.exh}$	energy utilization factors of secondary heat sources
β	pulse energy input factor
t_{WF_1}	temperature of the WF before the turbine, °C

Abbreviations

CII	Carbon intensity indicator
CO_2	Carbon dioxide
COM	Commission
EEXI	Existing energy efficiency index
EU	European Union
GHGs	Greenhouse gases
IMO	International Maritime Organization
LCA	Low-carbon-dioxide-generating fuel
MARPOL	The International Convention for the Prevention of Pollution from Ships
MEPC	The Marine Environment Protection Committee
ORC	Organic Rankine Cycle
SRC	Steam Rankine Cycle
RHE	Recuperative heat exchanger
WF	Working fluid
WHR	Waste heat recovery

Appendix A

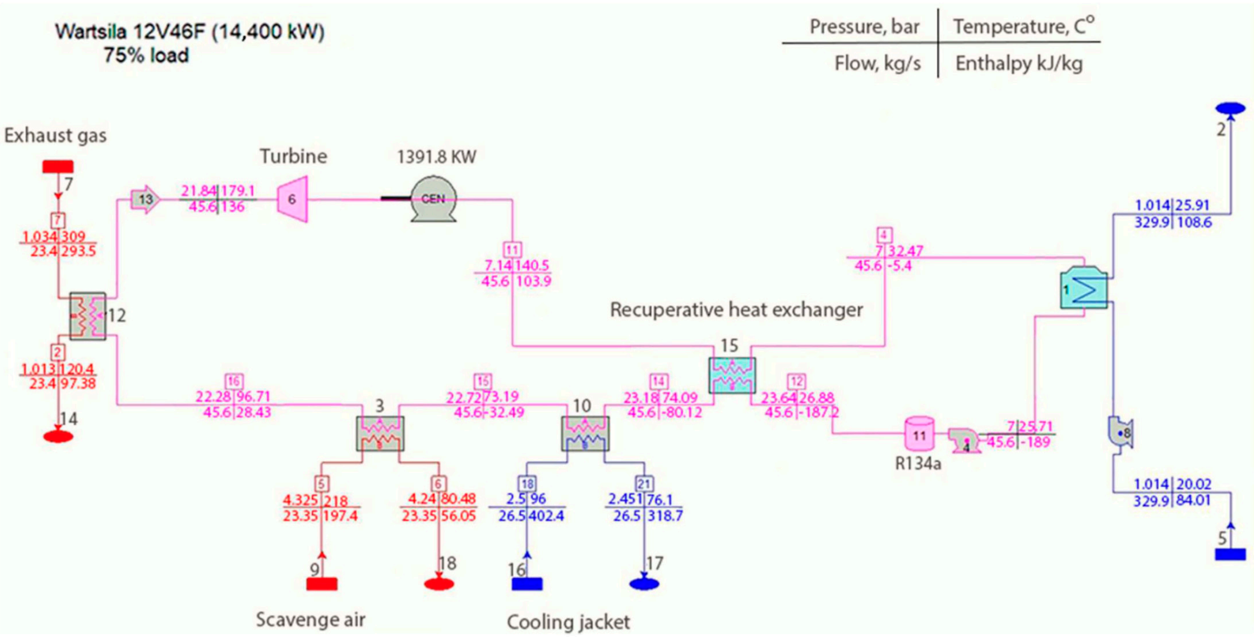

Figure A1. ORC–WHR cycle scheme implemented in thermal engineering software "Thermoflow".

Appendix B

Table A1. Research object "Wärtsila" 12V46F main engine general parameters.

Parameter	Data	Dimension
Manufacturer, type	WÄRTSILA 12V46, trunk type	-
Year of manufacture	2008	Year
Piston stroke	580	Mm
Average piston speed	9,7	m/s

Table A1. *Cont.*

Parameter	Data	Dimension
Cylinder diameter	460	mm
Number of cylinders	12	vnt.
Nominal power	12,000	kW
Possibility of reversal	Non-reversal	-
Type	4 stroke	-
Number of valves	48	pcs.
Crankshaftrevolutions	350–600	rpm
Type of fuel used	IFO 380 heavy fuel oil, diesel	-
Compression pressure	56	bar
Maximum combustion pressure	135	bar
Specific fuelconsumption	174	g/kWh

Table A2. Energy balance indicator calculation results.

	Load Mode %				
	100%	**85%**	**75%**	**50%**	**25%**
P_e, cil. kW	1200	1020	900	600	300
G_f, kg/s	0.72	0.59	0.55	0.38	0.20 *
η_e	0.469	0.483	0.459	0.44	0.425 *
$\propto_e$	2.5	2.68	298	3.38	3.8 *
G_{air}, kg/s	26.1	23.35	23.35	18.8	14.5 *
ρ_{air}, kg/m^3	4.51	4.26	4.44	4.1	3.98 *
P_K, bar	4.24	4.01	4.17	3.86	3.75
t_g, °C	366	316	309	273	255 *
$P_K{}'$, bar	4.45	4.2	4.38	4..06	3.93
$t_k{}'/c_p{}'$, °C	220 / 29.344	211 / 29.324	218 / 29.34	205 / 29.311	200 / 29.3
M_1, mol	1.25	1.34	1.49	1.69	1.9
M_{CO_2}, CO_2 kg fuel			0.0725		
M_{H_2O}, H_2O kg fuel			0.063		
M_{O_2}, O_2 kg fuel	0.156	0.174	0.206	0.248	0.291
M_{N_2}, N_2 kg fuel	0.99	1.06	1.18	1.338	1.51
M_2, mol	1.28	1.37	1.52	1.72	1.996
$mC_V{}'$, kj/kmolK			20.795		
$mC_p{}'$, kj/kmolK			29.11		
$mC_V{}''$, kj/kmolK	22.31	22.11	21.93	21.67	21.46
$mC_p{}''$, kj/kmolK	30.63	30.43	30.25	29.96	29.78
$Q_{exh.g.}$, kW	8990	6622	6622	4411	2387
Q_f, kW	30,744	25,193	23,485	16,226	8540
Q_e, kW	14,400	12,240	10,800	7200	3600
$Q_{sc.air}$, kW	4369	3629	3851	2814	1010
$Q_{cil} + Q_{oil}$, kW	2985	2702	2212	1801	1543
Q_{rad}, kW	420		Not applicable		

* extrapolation.

Table A3. Individual secondary heat source in ORC results.

Working Material	Load, %	Working Fluid Enthalpy (pos. 12), kJ/kg		Exhaust Gas Temperature (pos. 12), C		Working Material Temperature (pos. 6)		Working Fluid Enthalpy (pos. 6), kJ/kg		Working Material Flow, kg/s	Pressure, Bar (pos. 6)		Pressure Decrease Ratio (in Turbine, pos. 6)	Power, kW	Scavenge Air Temperature (pos.3)		Scavenge Air Flow, kg/s	Cylinder Cooling Temp. (poz 10)		Cylinder Cooling Flow, kg/s	η_e	$\delta\eta_{eRC}$	$\eta_{eRC_{cikl}}$	η_{RC}	$\Psi_{t.exh}$	$\Psi_{t.sc.air}$	$\Psi_{t.cil}$
EXHAUST GAS																											
R134a	100	−86.16	132.3	364	123.2	179.5	137.3	132.3	100.5	29.5	21.84	7.14	3.059	897.7	N/A		N/A	N/A		N/A	0.469	6.87%	0.48	0.142	0.994	N/A	N/A
	75	−86.17	132.3	309	121.5	175.9	137.3	132.3	100.5	20.3	21.84	7.14	3.059	613.6							0.459	6.25%		0.142	0.994		
	50	−86.18	132.3	273	121.3	175.9	137.3	132.3	100.5	13.15	21.84	7.14	3.059	367.7							0.44	5.66%		0.142	0.992		
	25	−86.16	132.3	255	121.7	175.9	137.3	132.3	100.5	8.9	21.84	7.14	3.059	248.7							0.425	7.65%		0.141	0.988		
SCAVENGE AIR																											
R134a	100	N/A		N/A		103.5	61.77	47.49	23.57	21	21.84	7.14	3.059	477.3	220	55.42	26.1	N/A		N/A	0.469	3.93%	0.47	0.263	N/A	0.9975	N/A
	75					103.2	61.38	47.06	23.19	18.6	21.84	7.14	3.059	422	218	55.08	23.35				0.459	4.46%		0.265		0.9995	
	50					105	63.37	49.27	25.17	13.7	21.84	7.14	3.059	313.8	205	55.64	18.8				0.44	4.91%		0.257		0.9958	
	25					105.5	63.92	49.87	25.71	10.2	21.84	7.14	3.059	234.3	200	55.72	14.5				0.425	7.25%		0.255		0.9951	
CYLINDER COOLING																											
R134a	100	N/A		N/A		87.62	43.9	27.55	5.815	15	21.84	7.14	3.059	309.9	N/A		N/A	96	75.26	35.7	0.469	2.76%	0.47	0.35889	N/A	N/A	0.988
	75					87.62	43.9	27.55	5.813	11	21.84	7.14	3.059	227.2				96	75.51	26.5	0.459	2.65%		0.35455			0.976
	50					87.62	43.89	27.54	5.81	9	21.84	7.14	3.059	185.9				96	75.33	21.5	0.44	3.13%		0.35784			0.984
	25					87.61	43.89	27.54	5.81	7.8	21.84	7.14	3.059	161.1				96	75.18	18.5	0.425	5.20%		0.36139			0.994

Table A4. Complex secondary heat source in ORC results.

Working Material	Load, %	Working Fluid Enthalpy (Pos. 12), kJ/kg		Exhaust Gas Temperature (Pos. 12), C		Working Material Temperature (Pos. 6)		Working Fluid Enthalpy (Pos. 6), kJ/kg		Working Material Flow, kg/s	Pressure, Bar (Pos. 6)		Pressure Decrease Ratio (in Turbine, Pos. 6)	Power, kW	Scavenge Air Temperature (Pos. 3)		Scavenge Air Flow, kg/s	Cylinder Cooling Temp. (Poz 10)		Cylinder Cooling Flow, kg/s	η_e	$\delta\eta_{eRC}$	$\eta_{eRC_{cikl}}$	η_{RC}	$\Psi_{t.exh}$	$\Psi_{t.sc.air}$	$\Psi_{t.cil}$
EXHAUST GAS + SCAVENGE AIR + CYLINDER COOLING																											
		Before	**After**	**Before**	**After**	**Before**	**After**	**Before**	**After**		**Before**	**After**			**Before**	**After**		**Before**	**After**								
R134a	*100*	28.76	135.7	364	120.5	178.8	140.3	135.7	103.6	60.4	21.84	7.14	3.059	1842.2	220	80.59	26.1	96	76.09	35.7	0.469	0.520	13.46%	0.132	0.996	0.846	0.948
	75	38.43	136	309	120.4	179.1	140.5	136	103.9	45.6	21.84	7.14		1391.8	218	80.48	23.35	96	76.1	26.5	0.459		13.49%	0.131	0.994	0.845	0.948
	50	47.19	136.3	273	120.1	179.3	140.7	136.3	104.2	32.5	21.84	7.14		992.7	205	79.82	18.8	96	76.1	21.5	0.44		14.39%	0.130	0.993	0.835	0.948
	25	55.55	136.5	255	120.6	179.5	140.9	136.5	104.4	24.2	21.84	7.14		739.6	200	79.57	14.5	96	76.09	18.5	0.425		21.39%	0.132	0.991	0.831	0.948
EXHAUST GAS + SCAVENGE AIR																											
R134a	*100*	72.29	178	364	120.3	178	139.4	134.8	102.8	46.9	21.84	7.14	3.059	1426.9	220	80.59	26.1	N/A			0.469	0.504	10.56%	0.133	0.996	0.846	N/A
	75	75.79	178.3	309	120.1	178.3	139.8	135.2	103.1	35.6	21.84	7.14	3.059	1084.2	218	80.48	23.35				0.459		10.63%	0.131	0.994	0.845	
	50	80.37	178.5	273	120.8	178.5	139.9	135.4	103.3	24.3	21.84	7.14	3.059	740.5	205	79.82	18.8				0.44		10.87%	0.130	0.993	0.835	
	25	83.79	178.6	255	120.5	178.6	140.1	135.5	103.4	17.2	21.84	7.14	3.059	524.3	200	79.57	14.5				0.425		15.36%	0.131	0.991	0.831	
EXHAUST GAS + CYLINDER COOLING																											
R134a	*100*	-12.1	134.5	364	120.3	177.8	139.2	134.5	102.5	44.1	21.84	7.14	3.059	1340.8				96	75.19	35.7	0.469	0.500	9.96%	0.141084	0.999	N/A	0.991
	75	-8.334	134.6	309	120.6	177.9	139.3	134.6	102.6	31.1	21.84	7.14	3.059	945.8				96	75.19	26.5	0.459		9.34%	0.140796	0.997		0.991
	50	3.048	135	273	120.5	178.2	139.6	135	102.9	21.9	21.84	7.14	3.059	666.6				96	75.19	21.5	0.44		9.84%	0.140583	0.997		0.991
	25	15.9	135.3	255	120.7	178.5	139.9	135.3	103.3	16.4	21.84	7.14	3.059	499.7				96	75.2	18.5	0.425		14.68%	0.1402	0.995		0.991
SCAVENGE AIR + CYLINDER COOLING																											
R134a	*100*					170.7	132	126.2	94.9	31	21.84	7.14	3.059	921.9	220	83.14	26.1	96	75.19	35.7	0.469	0.490	7.04%	0.132168	N/A	0.831	0.991
	75					152.4	113.3	104.9	75.5	26	21.84	7.14	3.059	727.6	218	79.63	23.35	96	75.19	26.5	0.459		7.31%	0.14799		0.850	0.991
	50					176.8	138.2	133.4	101.5	17	21.84	7.14	3.059	515.3	205	79.89	18.8	96	75.19	21.5	0.44		7.73%	0.112181		0.645	0.991
	25					177	138.4	133.6	101.7	14	21.84	7.14	3.059	424.7	200	79.23	14.5	96	75.19	18.5	0.425		12.58%	0.124063		0.680	0.991

References

1. MARPOL Annex VI, Resolution MEPC.308(73). 2018. Available online: https://wwwcdn.imo.org/localresources/en/KnowledgeCentre/IndexofIMOResolutions/MEPCDocuments/MEPC.308(73).pdf (accessed on 23 July 2024).
2. International Maritime Organization (IMO). Third IMO Greenhouse Gas Study 2014. Available online: https://www.imo.org/en/OurWork/Environment/Pages/Greenhouse-Gas-Studies-2014.aspx (accessed on 9 November 2023).
3. Maritime Industry Authority. MARPOL 73/78. 1973. Available online: https://marina.gov.ph/wp-content/uploads/2020/10/MARPOL-73_78.pdf (accessed on 23 July 2024).
4. Guidelines on Survey and Certification of the Attained Energy Efficiency Existing Ship Index (EEXI), Resolution MEPC.351(78). 2022. Available online: https://wwwcdn.imo.org/localresources/en/KnowledgeCentre/IndexofIMOResolutions/MEPCDocuments/MEPC.351(78).pdf (accessed on 23 July 2024).
5. Interim Guidelines on Correction Factors and Voyage Adjustments for CII Calculations, Resolution MEPC.355(78). 2022. Available online: https://wwwcdn.imo.org/localresources/en/KnowledgeCentre/IndexofIMOResolutions/MEPCDocuments/MEPC.355(78).pdf (accessed on 23 July 2024).
6. United Nations Framework Convention on Climate Change (UNFCCC). World Trade and the Reduction of CO2 Emissions, International Chamber of Shipping. 2014. Available online: https://www.ics-shipping.org (accessed on 23 November 2023).
7. EU Monitor. Use of Renewable and Low-Carbon Fuels in Maritime Transport. *COM* **2021**, *562*. Available online: https://www.europarl.europa.eu/RegData/docs_autres_institutions/commission_europeenne/com/2021/0551/COM_COM(2021)0551_EN.pdf (accessed on 23 July 2024).
8. EU Monitor. Directive of the European Parliament and of the Council. *COM* **2021**, 551.
9. International Chamber of Shipping (ICS). Getting to Zero Coalition: Exploring Pathways to Decarbonization in Shipping. 2020. Available online: https://globalmaritimeforum.org/getting-to-zero-coalition/ (accessed on 23 July 2024).
10. Maersk Mc-Kinney Moller Center for Zero Carbon Shipping. The Shipping Industry's Fuel Choices on the Path to Net Zero. 2023. Available online: https://www.globalmaritimeforum.org/ (accessed on 1 December 2023).
11. Fisher, R.; Ciappi, L.; Niknam, P.; Braimakis, K.; Karellas, S.; Frazzica, A.; Sciacovelli, A. Innovative waste heat valorisation technologies for zero-carbon ships. A review. *Appl. Therm. Eng.* **2024**, *253*, 123740. [CrossRef]
12. Bellolio Domke, S.A.; Lemort, V.; Rigo, P. Organic Rankine cycles systems for waste heat recovery in marine applications. In Proceedings of the International Conference on Shipping in Changing Climates, SCC 2015, Glasgow, UK, 24–26 November 2015.
13. Theotokatos, G.; Livanos, G.A. Techno-economic analysis of single pressure exhaust gas waste heat recovery systems in marine propulsion plants. *Proc. Inst. Mech. Eng. Part M J. Eng. Marit. Environ.* **2013**, *227*, 83–97.
14. Ouyang, T.; Su, Z.; Yang, R.; Li, C.; Huang, H.; Wei, Q. A framework for evaluating and optimizing the cascade utilization of medium-low grade waste heat in marine dual-fuel engines. *J. Clean. Prod.* **2020**, *276*, 123289. [CrossRef]
15. Dimopoulos, G.; Georgopoulou, C.; Kakalis, N. Modelling and optimization of an integrated marine combined cycle system. In Proceedings of the 24th International Conference on Energy, Cost, Optimization, Simulation and Environmental Impact of Energy Systems (ECOS), Novi Sad, Serbia, 4–7 July 2011; pp. 1283–1298.
16. Hountalas, D.; Katsanos, C.; Mavropoulos, G. Efficiency improvement of large scale 2-stroke diesel engines through the recovery of exhaust gas using a rankine cycle. *Procedia-Soc. Behav. Sci.* **2012**, *48*, 1444–1453. [CrossRef]
17. Duong, P.A.; Ryu, B.; Lee, H.; Kang, H. Thermodynamic analysis of integrated ammonia fuel cells system for maritime application. *Energy Rep.* **2023**, *10*, 1521–1537. [CrossRef]
18. Altosole, M. Waste heat recovery systems from marine diesel engines: Comparison between new design and retrofitting solutions. In *Maritime Technology and Engineering*; CRC Press: Boca Raton, FL, USA, 2014; pp. 735–742.
19. Díaz-Secades, L.; González, R.; Rivera, N.; Montañés, E.; Quevedo, J.R. Waste heat recovery system for marine engines optimized through a preference learning rank function embedded into a Bayesian optimizer. *Ocean. Eng.* **2023**, *281*, 114747. [CrossRef]
20. Zebroski, E. Industrial and Commercial Cogeneration. In *Annual Report to the Congress for 1982 (March 1983)*; 1983. Available online: https://swh.princeton.edu/~ota/disk3/1983/9565/9565.PDF (accessed on 23 July 2024).
21. Hatchman, J.C. Steam cycles for waste heat recovery: A case study. *R&D J.* **1991**, *7*, 32–38.
22. Casisi, M.; Pinamonti, P.; Reini, M. Increasing the energy efficiency of an internal combustion engine for ship propulsion with bottom ORCS. *Appl. Sci.* **2020**, *10*, 6919. [CrossRef]
23. Konur, O.; Yuksel, O.; Korkmaz, S.; Aykut, S.; Colpan, C.; Saatçioğlu, O.; Yaşar, Ö.; Koseoglu, B. Operation-Dependent Exergetic Sustainability Assessment and Environmental. *Energy* **2023**, *262*, 125477. [CrossRef]
24. Vaja, I.; Gambarotta, A. Internal Combustion Engine (ICE) Bottoming with Organic Rankine Cycle (ORCs). *Energy* **2010**, *35*, 2387–2399. [CrossRef]
25. Teng, H.; Regner, G.; Cowland, C. *Waste Heat Recovery of Heavy-Duty Diesel Engines by Organic Rankine Cycle Part I: Hybrid Energy System of Diesel and Rankine Engines*; SAE Technical Paper 2007-01-0537; SAE International: Warrendale, PA, USA, 2007. [CrossRef]
26. Grljušić, M.; Medica, V.; Račić, N. Thermodynamic Analysis of a Ship Power Plant Operating with Waste Heat Recovery through Combined Heat and Power Production. *Energies* **2014**, *7*, 7368–7394. [CrossRef]
27. Song, J.; Song, Y.; Gu, C. Thermodynamic and lysis and performance optimization of an Organic Rankine Cycle (ORC) waste heat recovery system for marine diesel engines. *Energy* **2015**, *82*, 976–985. [CrossRef]
28. Pantano, F.; Capata, R. Expander Selection for an on board ORC energy recovery system. *Energy* **2017**, *141*, 1084–1096. [CrossRef]

29. Ouyang, T.; Huang, G.; Lu, Y.; Liu, B.; Hu, X. Multi-criteria assessment and optimization of waste heat recovery for large marine diesel engines. *J. Clean. Prod.* **2021**, *309*, 127307. [CrossRef]
30. Ng, C.W.; Tam, I.C.K.; Wu, D. *Study of a Waste Energy Driven Organic Rankine Cycle Using Free Piston Linear Expander for Marine Application*; The National Technical University of Athens: Athens, Greece, 2019.
31. Park, B.S.; Usman, M.; Imran, M.; Pesyridis, A. Review of Organic Rankine Cycle experimental data trends. *Energy Convers. Manag.* **2018**, *173*, 679–691. [CrossRef]
32. Baldi, F.; Larsen, U.; Gabrielii, C. Comparison of different procedures for the optimisation of a combined diesel engine and organic Rankine cycle system based on ship operational profile. *Ocean Eng.* **2015**, *110*, 85–93. [CrossRef]
33. Konur, O.; Yuksel, O.; Korkmaz, S.; Aykut, S.; Colpan, C.; Saatçioğlu, O.; Yaşar, Ö.; Koseoglu, B. Operation-Dependent Exergetic Sustainability Assessment and Environmental Analysis on a Large Tanker Ship Utilizing Organic Rankine Cycle System. *SSRN* 2022. [CrossRef]
34. Akman, M.; Ergin, S. Thermo-environmental analysis and performance optimisation of transcritical organic Rankine cycle system for waste heat recovery of a marine diesel engine. *Ships Offshore Struct.* **2020**, *16*, 1104–1113. [CrossRef]
35. Ng, C. Modelling and Simulation of Organic Rankine Cycle Waste Heat Recovery System with the Operational Profile of a Ship. Ph.D. Thesis, Newcastle University, Newcastle upon Tyne, UK, 2021.
36. Ng, C.; Tam, I.C.K.; Wetenhall, B. Waste Heat Source Profiles for Marine Application of Organic Rankine Cycle. *J. Mar. Sci. Eng.* **2022**, *10*, 1122. [CrossRef]
37. Qu, J.; Feng, Y.; Zhu, Y.; Zhou, S.; Zhang, W. Design and thermodynamic analysis of a combined system including steam Rankine cycle, organic Rankine cycle, and power turbine for marine low-speed diesel engine waste heat recovery. *Energy Convers. Manag.* **2021**, *245*, 114580. [CrossRef]
38. Baldasso, E.; Mondejar, M.E.; Andreasen, J.G.; Rønnenfelt, K.A.T.; Nielsen, B.Ø.; Haglind, F. Design of organic Rankine cycle power systems for maritime applications accounting for engine backpressure effects. *Appl. Therm. Eng.* **2020**, *178*, 115527. [CrossRef]
39. Liu, X.; Nguyen, M.; Chu, J.; Lan, T.; He, M. A novel waste heat recovery system combing steam Rankine cycle and organic Rankine cycle for marine engine. *J. Clean. Prod.* **2020**, *265*, 121502. [CrossRef]
40. Ng, C.; Tam, I.C.K.; Wu, D. Thermo-Economic Performance of an Organic Rankine Cycle System Recovering Waste Heat Onboard an Offshore Service Vessel. *J. Mar. Sci. Eng.* **2020**, *8*, 351. [CrossRef]
41. Kim, D.; Lee, J.; Kim, J.; Kim, M.; Kim, M. Parametric study and performance evaluation of an organic Rankine cycle (ORC) system using low-grade heat at temperatures below 80 °C. *Appl. Energy* **2017**, *189*, 55–65. [CrossRef]
42. Grljusic, M.; Medicav, R.; Radica, G. Calculation of efficiencies of a ship power plant operating with waste heat recovery through combined heat and power production. *Energies* **2015**, *8*, 4273–4299. [CrossRef]
43. Sung, T.; Kim, K.C. Thermodynamic analysis of a novel dual-loop organic Rankine cycle for engine waste heat and LNG cold. *Appl. Therm. Eng.* **2016**, *100*, 1031–1041. [CrossRef]
44. Luo, W.H.; Chen, W.; Jiang, A.G.; Tian, Z. Comparative analysis of thermodynamics performances of ORC systems recovering waste heat from ship diesel engines. *China Mech. Eng.* **2022**, *33*, 452–458.
45. Shu, G.; Liu, P.; Tian, H.; Wang, X.; Jing, D. Operational profile based thermal-economic analysis on an Organic Rankine cycle using for harvesting marine engine's exhaust waste heat. *Energy Convers. Manag.* **2017**, *146*, 107–123. [CrossRef]
46. Sellers, C. Field operation of 125kW ORC with ship engine jacket water. *Energy Procedia* **2017**, *129*, 495–502. [CrossRef]
47. Ouyang, T.; Su, Z.; Zhao, Z.; Wang, Z.; Huang, H. Advanced exergo-economic schemes and optimization for medium–low grade waste heat recovery of marine dual-fuel engine integrated with accumulator. *Energy Convers. Manag.* **2020**, *226*, 113577. [CrossRef]
48. Su, Z.; Ouyang, T.; Chen, J.; Xu, P.; Tan, J.; Chen, N.; Huang, H. Green and efficient configuration of integrated waste heat and cold energy recovery for marine. *Energy Convers. Manag.* **2020**, *209*, 112650. [CrossRef]
49. Pesyridis, A.; Asif, M.S.; Mehranfar, S.; Mahmoudzadeh Andwari, A.; Gharehghani, A.; Megaritis, T. Design of the Organic Rankine Cycle for High-Efficiency Diesel Engines in Marine Applications. *Energies* **2023**, *16*, 4374. [CrossRef]
50. Elkafas, A.G. Thermodynamic Analysis and Economic Assessment of Organic Rankine Cycle Integrated with Thermoelectric Generator Onboard Container Ship. *Processes* **2024**, *12*, 355. [CrossRef]
51. Niknam, P.H.; Fisher, R.; Ciappi, L.; Sciacovelli, A. Optimally integrated waste heat recovery through combined emerging thermal technologies: Modelling, optimization and assessment for onboard multi-energy systems. *Appl. Energy* **2024**, *366*, 123298. [CrossRef]
52. Duong, P.A.; Ryu, B.R.; Song, M.K.; Nam, D.; Kang, H. Thermodynamics analysis of a novel designation of LNG solid oxide fuel cells combined system with CO_2 capture using LNG cold energy. *J. Eng. Res.* **2024**, *12*, 226–238. [CrossRef]
53. *ISO 8178-1:2006*; Reciprocating Internal Combustion Engines—Exhaust Emission Measurement. International Organization for Standardization: Geneva, Switzerland, 2006.
54. Lebedevas, S.; Čepaitis, T. Complex Use of the Main Marine Diesel Engine High- and Low-Temperature Waste Heat in the Organic Rankine Cycle. *J. Mar. Sci. Eng.* **2024**, *12*, 521. [CrossRef]

55. Lebedevas, S.; Čepaitis, T. Research of Organic Rankine Cycle Energy Characteristics at Operating Modes of Marine Diesel Engine. *J. Mar. Sci. Eng.* **2021**, *9*, 1049. [CrossRef]
56. Mohammed, A.; Mosleh, M.; El-Maghlany, W.; Ammar, N. Performance analysis of supercritical ORC utilizing marine diesel engine waste heat recovery. *Alex. Eng. J.* **2020**, *59*, 893–904. [CrossRef]